

Filipstadite, a new Mn-Fe³⁺-Sb derivative of spinel, from Långban, Sweden

PETE J. DUNN

Department of Mineral Sciences, Smithsonian Institution, Washington, D.C. 20560, U.S.A.

DONALD R. PEACOR

Department of Geological Sciences, University of Michigan, Ann Arbor, Michigan 48109, U.S.A.

ALAN J. CRIDDLE, CHRIS J. STANLEY

Department of Mineralogy, The British Museum (Natural History), Cromwell Road, London, SW7 5BD, England

ABSTRACT

Filipstadite, (Mn,Mg)₂(Sb_{0.5}⁵⁺Fe_{0.5}³⁺)O₄ is a new mineral, related to spinel, from Långban, Värmland, Sweden. Filipstadite is orthorhombic, pseudocubic, with $A = 8.640$ Å for its cubic subcell. The strongest reflections in the X-ray powder pattern are [$d(I/I_0)(hkl)$] 2.56 (100) (311), 1.527 (70) (440), 1.662 (60) (511), and 2.157 (40) (400). Filipstadite is black and occurs as equant crystals intimately associated with ingersonite, jacobsonite, and calcite. In polished section (~3200 K) it is gray, and for illuminant C, depending on composition, Y varies from 11.4 to 12.3%, λ_d from 473 to 475 nm and P_e from 2.3 to 3.3%. It is weakly anisotropic with poorly developed sector twinning.

INTRODUCTION

During the characterization of ingersonite, a new Ca-Mn antimonate mineral from Långban, Sweden (Dunn et al., 1988), we noted an opaque mineral with X-ray diffraction and chemical characteristics suggesting that it is related to, yet distinct from, spinels. Our subsequent investigation of this mineral has shown it to be a new species, related to spinel, with Fe³⁺ and Sb⁵⁺ apparently ordered over octahedrally coordinated sites. We have named this new mineral *filipstadite* for the city of Filipstad, in Sweden, near which the Långban mine is located. The new mineral and the name were approved by the Commission on New Minerals and Mineral Names, IMA. Holotype material is preserved at the Smithsonian Institution under catalogue number NMNH 163012 and at the British Museum (Natural History) under catalogue number BM 1986, 410: E.1177 and BM 1986, 411: E.1178.

OCCURRENCE

Filipstadite is known to us from only one specimen, which is also the holotype specimen for ingersonite. It was found on the dumps of the Långban mine, near Filipstad, Värmland, Sweden, and was called to our attention by Roland Eriksson of Långban. Filipstadite occurs as euhedral crystals up to 200 μ m in diameter, occurring singly and in aggregates, and intimately associated with jacobsonite, ingersonite, and calcite (Dunn et al., 1988). Textural relations are given below. Other associated minerals are antimony (verified optically and by microprobe) and a magnesium silicate, probably clinohumite.

X-RAY CRYSTALLOGRAPHY

Filipstadite was studied using Weissenberg and precession methods. The diffuse photographs show a substructure-superstructure relationship (Fig. 1), with intense reflections corresponding to the diffraction pattern of spinel, although the d -glide extinction rule of spinel is violated by weak reflections. These relationships imply that the space group of filipstadite is a subgroup of that of spinel. Most single crystals give rise to complex reflections that suggest imperfect crystals with mosaic structure. It is not possible to deduce definitive symmetry relations for such crystals. However, one crystal displayed sharp reflections that showed that (1) there is no threefold axis; (2) there is no fourfold axis and only one of the fourfold axes of spinel is a twofold axis in filipstadite; (3) the Laue symmetry is $2/m\ 2/m\ 2/m$, and filipstadite is therefore orthorhombic, with a , b , and c of filipstadite being parallel to [110], [1 $\bar{1}$ 0], and [001] of spinel, respectively. It is of interest to point out that the low-temperature form of Fe₃O₄ has an analogous relationship to magnetite (Hamilton, 1958).

The choice of axes defined by these relationships gives rise to the lattice parameters $a = 3\sqrt{2}A = 36.7$ Å, $b = 3\sqrt{2}A = 36.7$ Å, and $c = 3A = 25.9$ Å, where A is the unit-cell translation of spinel. These axes have the same directions as those in the low-temperature form of magnetite, for which $a = 1/\sqrt{2}A = 5.91$ Å, $b = 1/\sqrt{2}A = 5.93$ Å, and $c = A = 8.39$ Å. Definition of this unit cell gives rise to a complex pattern of non-space-group extinction rules, which prevent definition of space-group symmetry elements in the usual fashion. The problem is exacerbated by the paucity of observable superstructure

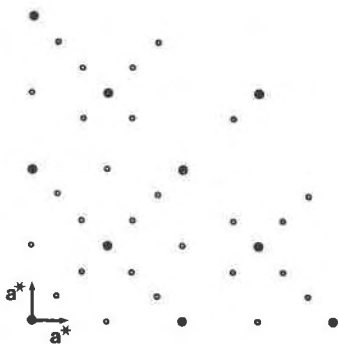


Fig. 1. Pattern of observed reflections in the $hk0$ net. The a^* axis is shown for the cubic spinel unit cell. Large solid circles correspond to reflections occurring in the spinel diffraction pattern. Small open circles are superstructure reflections. Some of these (e.g., 200 and 600, indexed on the cubic spinel unit cell) correspond to extinct reflections (d glide) in the cubic spinel diffraction pattern. Although intensity relationships are not evident in the figure, diffraction patterns display mirror planes along $[110]^*$ and $[1\bar{1}0]^*$, but not along a^* .

reflections. Attempts to improve the definition of diffraction relations included obtaining photographs in a wide variety of orientations, using $\text{CuK}\alpha$ radiation for precession photographs (in order to guarantee level resolution in light of the large lattice parameters), and using a variety of crystals. In the latter case, all except the one yielding sharp reflections gave rise to cubic symmetry, as determined using imperfect reflections, implying the existence of twinning. This is to be expected in such a substructure-superstructure relation, and it was confirmed by optical studies (see below). Lastly, photographs in orientations that are symmetry-equivalent in spinel, but not in filipstadite, were directly compared in order to

detect dimensional deviations from those required by cubic symmetry. None was detected.

These relationships demonstrate that filipstadite is not cubic, but has a structure that is derived from that of spinel. Because the single-crystal relations give rise to an extraordinarily large unit cell and non-space-group extinctions, without firm designation of space group, the unit cell defined here must be considered to be tentative. The powder diffraction data, obtained using a polycrystalline sample, $\text{FeK}\alpha$ radiation, and a Gandolfi 114.6-mm diameter camera (Table 1), are therefore indexed only for the cubic substructure reflections, although comparison of d values of superstructure reflections occurring in the powder and single-crystal patterns shows excellent correspondence. Least-squares refinement of data for substructure reflections gives rise to $A = 8.640(1)$ Å, for the cubic subcell.

Hamilton (1958) showed that the low-temperature form of magnetite has equal numbers of Fe^{2+} and Fe^{3+} on octahedral sites and Fe^{3+} and Fe^{2+} ordered on those sites, such that rows of Fe^{3+} and Fe^{2+} ions extend parallel to a and b , respectively ($a = 1/\sqrt{2}A$, $b = 1/\sqrt{2}A$, $c = A$, where A is the cubic lattice parameter). The substructure-superstructure relationship between spinel and filipstadite implies that filipstadite has a structure that is derivative to that of spinel. Such relations may be due to ordered, low-symmetry distortions or to ordered substitutions. Because the formula has nearly equal numbers of Sb^{5+} and Fe^{3+} inferred to be on the octahedral sites (see below) and because of the analogy to magnetite, we tentatively conclude that in filipstadite, the superstructure may be caused by Sb^{5+} - Fe^{3+} ordering.

Observations in reflected light (see below) show that many filipstadite crystals have cores of jacobsonite, implying that the single crystals or powdered samples used for

TABLE 1. Powder-diffraction data for filipstadite

hkl	d_{obs}	d_{calc}	hkl	d_{obs}	d_{calc}	hkl
20	4.97	4.99	111	60	1.662	511
2	4.59*					333
5	4.38	4.32	200**	70	1.527	440
15	3.90*			5	1.461	531
5	3.37*			2	1.420*	
30	3.05	3.05	220	2	1.369	620
100	2.56	2.61	311	1	1.347*	
10	2.49	2.49	222	20	1.318	533
2	2.261*			10	1.304	622
1	2.185*			1	1.269*	
40	2.157	2.160	400	2	1.2095	551
1	1.979	1.982	331			711
5	1.763	1.764	422	5	1.1545	642
2	1.726*			30	1.1251	731
2	1.686*					553
				5	1.0811	800
				10	0.9977	751
						555
				5	0.9916	662
						662

Note: Data obtained using a 114.6-mm-diameter Gandolfi camera, $\text{FeK}\alpha$ radiation, and Si as an internal standard. Calculated d values obtained using $a = 8.640$ Å. Intensities visually estimated.

* Superstructure reflection.

** Reflection extinct in spinel.

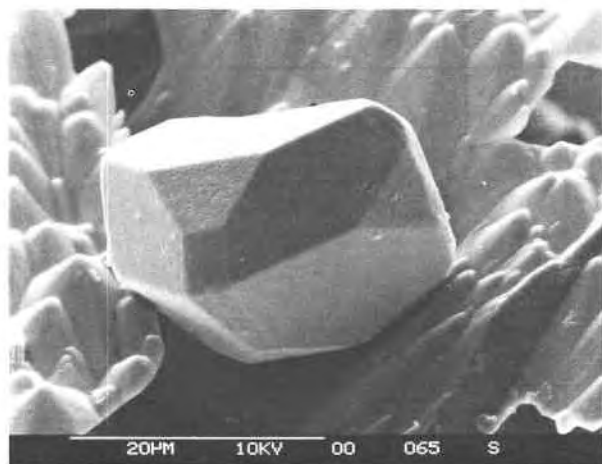


Fig. 2. Euhedral crystals of filipstadite showing forms equivalent to two cubic forms, the octahedron and dodecahedron. Scale bar is 20 μm .

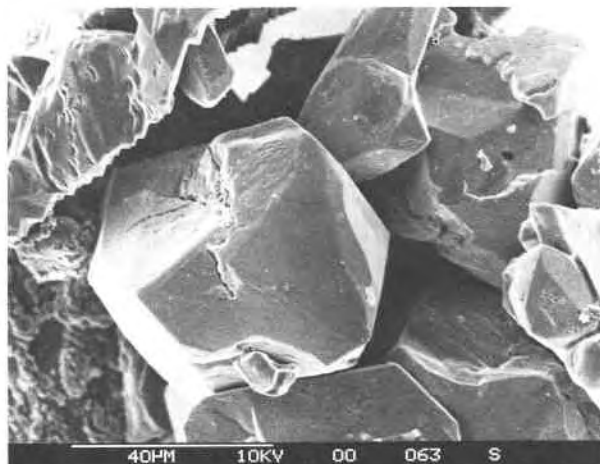


Fig. 3. Irregular filipstadite crystals in an aggregate, with platy ingersonite. Scale bar is 40 μm .

X-ray diffraction studies may have had a contribution from jacobsite. Because jacobsite has a lattice parameter significantly smaller [$a \approx 8.5 \text{ \AA}$ according to Katz (1960)] than that of the filipstadite subcell, mixtures of the two minerals should result in a doubling of high-theta reflections. None was observed, and the X-ray diffraction data are therefore inferred to be free of a contribution from jacobsite.

PHYSICAL AND OPTICAL DESCRIPTION

Filipstadite forms euhedral to subhedral crystals, up to 200 μm in diameter, which are predominantly apparently octahedral in habit, with dodecahedral and possibly cubic modifications. These crystals occur both as isolated euhedra within calcite (Fig. 2) and as more irregular crystals in aggregates (Fig. 3). Filipstadite is black in hand specimen, with a brown streak, metallic luster, no apparent cleavage, and a conchoidal fracture, and is brittle. The hardness is $\text{VHN}_{100} = 831 \text{ kg/mm}^2$ (range = 792–882). The density could not be measured because of the small grain size and the presence of irregular cores of jacobsite, as discussed below. The calculated density is 4.9 g/cm^3 .

In polished section, filipstadite is seen to be closely associated and intergrown with ingersonite (Dunn et al., 1988) and jacobsite, which it partly replaces. Aggregates up to 2 mm across of intergrown filipstadite crystals are common, and individual crystals, for the most part, retain their angular outlines. Minute inclusions (5–10 μm) of native antimony were observed in the calcite matrix. In plane-polarized light, growth zonation of filipstadite is apparent, particularly where the mineral overgrows or replaces grains of jacobsite. The growth zonation is clearly related to composition. A typical feature is a rim (up to 50 μm) of filipstadite (Table 2, analysis 5; Fig. 4) around a core of euhedral jacobsite (white and more reflective in this assemblage). In some instances, this rim is overgrown by slightly darker filipstadite. Where filipstadite

has clearly replaced jacobsite, it commonly displays a gradual zonation, in which (Fig. 5) individual zones are not sharply defined. The most abundant grains of filipstadite are, however, compositionally homogeneous and have the same composition as the midgray filipstadite (Table 2, analyses 1–4).

Filipstadite is not visibly bireflectant, but, between crossed polars, the mineral is weakly anisotropic, with rotation tints in shades of dark brownish gray. With the polars uncrossed by 3° , the anisotropic effects are enhanced and reveal that successive zones of the mineral were deposited in slightly different crystallographic orientations. Poorly developed sector twinning is not uncommon. Internal reflections are rare (the mineral is opaque) except at grain boundaries where, in some grains, amber and brownish or red internal reflections occur; these reflections are more apparent in oil immersion. Immersion has no effect other than to reduce the reflectance of the mineral. Filipstadite polishes perfectly and has a high polishing hardness, similar to that of jacobsite and clinohumite(?), and greater than that of ingersonite and calcite.

TABLE 2. Electron-microprobe analyses (wt%) of filipstadite

No.	SiO ₂	Al ₂ O ₃	MgO	MnO	Fe ₂ O ₃	Sb ₂ O ₅	Total
1	0.2	0.6	12.3	36.8	15.3	34.8	100.0
2	0.1	0.5	11.7	36.6	16.6	33.5	99.0
3	0.3	0.7	11.9	36.8	15.4	34.1	99.2
4	0.2	1.3	11.6	39.0	13.5	34.4	100.0
5	0.2	0.3	14.4	32.3	22.4	31.4	101.0
6	0.8	0.3	14.9	34.8	13.8	34.5	99.1

Note: Instrument: Cambridge Instruments Microscan IX. Operating conditions: Accelerating voltage 20 kV; beam current 2.50×10^{-8} A on Faraday cup. Standards: MgCr_2O_4 (Mg), wollastonite (Si, Al), and pure metals (Mn, Sb, Fe). Radiations measured: $\text{SiK}\alpha$, $\text{AlK}\alpha$, $\text{MgK}\alpha$, $\text{MnK}\alpha$, $\text{FeK}\alpha$, and $\text{SbL}\alpha$.

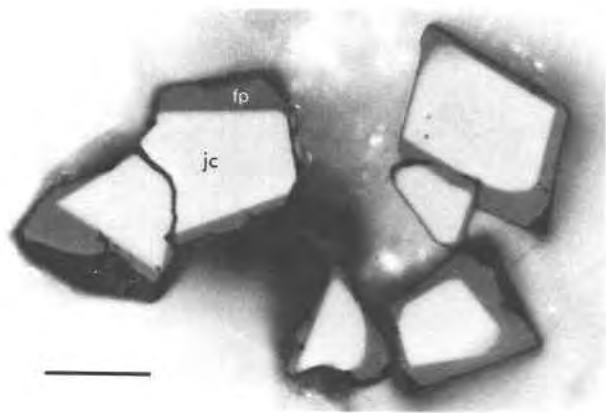


Fig. 4. Reflected-light photomicrograph of isolated grains of jacobsite (jc) overgrown by filipstadite (fp) in calcite matrix (oil immersion). Scale bar is 35 μm .

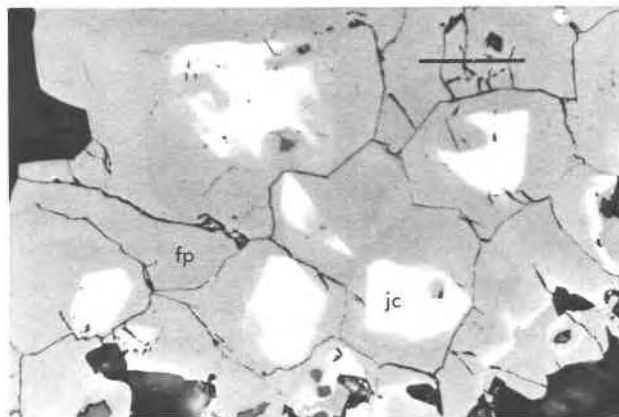


Fig. 5. Reflected-light photomicrograph illustrating subhedral to anhedral partially replaced grains of jacobsite (jc) overgrown by subtly zoned filipstadite (fp) aggregates. Scale bar is 55 μm .

REFLECTANCE DATA, COLOR VALUES, AND OPTICAL CONSTANTS

Reflectance measurements were made on six different grains of filipstadite, five on grains in matrix in polished mount E.1177 and the other on a single grain (in polished mount E.1178) that had previously been used in the X-ray study. The polishing and measurement procedures were as described by Criddle et al. (1983). The reflectance standard used was SiC (Zeiss no. 472), and measurements were made with $\times 16$ air and oil objectives (effective numerical aperture 0.15). Zeiss oil (N_D 1.515) was used for the immersion measurements at 20 $^{\circ}\text{C}$.

The grains measured were the same as those analyzed by electron microprobe, and the numbers used in the table of analyses (Table 2) correspond to those used in the tables of reflectance data (Tables 3¹ and 4). Filipstadite is

¹ A copy of Tables 3 and 6 may be ordered as Document AM-88-366 from the Business Office, Mineralogical Society of America, 1625 I Street, N.W., Suite 414, Washington, D.C. 20006, U.S.A. Please remit \$5.00 in advance for the microfiche.

not perceptibly bireflectant, but, of the six areas measured, four were anisotropic: minimum and maximum reflectances (R_1 and R_2 , respectively) were obtained for these grains. It will be recalled that, immediately adjacent to jacobsite, filipstadite sometimes forms a thin rim with a slightly higher reflectance than the "bulk" filipstadite; this was confirmed by measurement of one such rim, grain 5 in Tables 3 and 4. All of the spectra measured are concordant (Fig. 6) and weakly dispersed; those of grains 1 to 4 differ from one another by less than the generally accepted measurement error for reflectance measurements ($\pm 0.5\%$). This is also the case for grain 6; however, the reflectances of this grain are consistently lower. Color values (Table 5) were calculated from the reflectance data for grains 2, 5, and 6 (grain 2 being taken as representative of grains 1 to 4) relative to CIE illuminants C and A, at 6774 K and 2856 K, respectively. The similarity in the dominant wavelengths, λ_d (corresponding in subjective terminology to the hue), and in the excitation purities P_e (%), corresponding to the saturation) of the three grains (Table 2) underlines the consistency of the dispersion of

TABLE 4. Partial reflectance data for filipstadite

λ (nm)	1		2		3		4		5		6	
	R'	R_1	R_2	R_1	R_2	R_1	R_2	R_1	R_2	R'	R_1	R_2
400	12.8	12.7	12.9	12.8	13.0	12.8	12.8	13.7	12.45	12.5	12.3	
420	12.5	12.5	12.7	12.5	12.7	12.6	12.6	13.4	12.2	12.3	12.1	
440	12.4	12.3	12.5	12.3	12.5	12.4	12.4	13.2	12.0	12.1	12.0	
460	12.2	12.1	12.3	12.1	12.3	12.2	12.2	13.0	11.85	12.0	12.0	
480	12.0	12.0	12.2	11.9	12.1	12.0	12.0	12.8	11.7	11.8	11.8	
500	11.9	11.9	12.1	11.8	12.0	11.9	11.9	12.6	11.6	11.7	11.7	
520	11.8	11.8	12.0	11.7	11.85	11.8	11.8	12.5	11.5	11.65	11.65	
540	11.7	11.7	11.9	11.6	11.8	11.7	11.7	12.3	11.4	11.6	11.6	
560	11.65	11.65	11.8	11.6	11.7	11.6	11.6	12.2	11.35	11.5	11.5	
580	11.6	11.6	11.7	11.55	11.6	11.5	11.6	12.1	11.3	11.45	11.45	
600	11.6	11.6	11.7	11.5	11.6	11.5	11.5	12.1	11.3	11.4	11.4	
620	11.6	11.6	11.7	11.5	11.6	11.45	11.5	12.0	11.3	11.4	11.4	
640	11.5	11.5	11.7	11.5	11.6	11.4	11.5	12.0	11.2	11.4	11.4	
660	11.5	11.5	11.6	11.4	11.55	11.4	11.4	12.0	11.2	11.3	11.3	
680	11.45	11.4	11.6	11.4	11.5	11.35	11.4	11.95	11.2	11.3	11.3	
700	11.4	11.4	11.5	11.4	11.5	11.3	11.35	11.85	11.15	11.3	11.3	

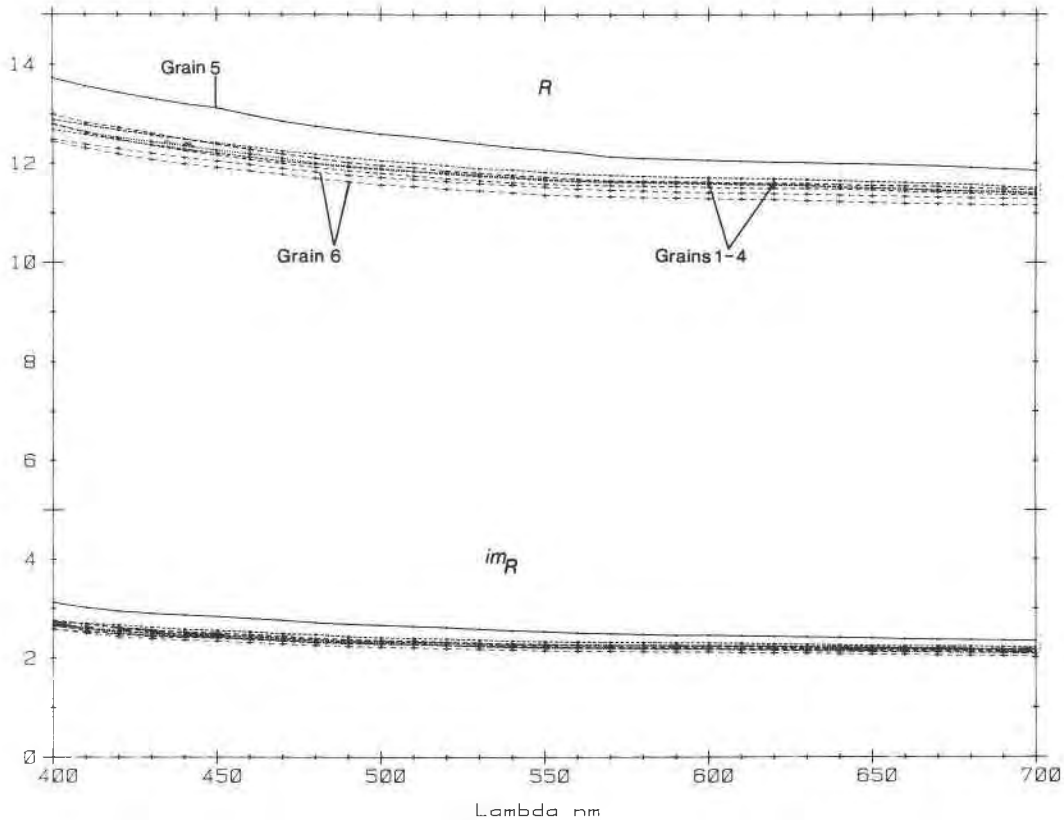


Fig. 6. Reflectance spectra in air (R) and oil immersion (mR).

their reflectance. However, the luminance values [Y (%)] clearly show the differences in reflectance between the three grains, differences that must be compared with the variations in composition of these grains (Table 2). Grain 5 has a higher Fe and Mg content, and a lower Mn and Sb content, than grains 1 to 4 and has a higher reflectance. Grain 6, the lowest-reflecting grain, has a higher Si and Mg content; its Sb and Fe content is broadly similar to those of grains 1 to 4, and its Mn content falls between that of grain 5 and grains 1 to 4. It is obvious, therefore, that the reflectance spectra are influenced by the composition of the mineral, but it is not obvious, from the

few data available and the number of specimens involved, precisely how the reflectance is controlled.

The reflectance data were used to compute the indices of refraction (n) and absorption coefficients (k) of filipstadite by means of the two-media method with the Koenigsberger equations. It will be seen (Fig. 7) that the indices of refraction are little dispersed, with $r < v$. The similarity of the dispersion of the n and R spectra is noticeable, suggesting that n rather than k is more significant in determining R . The absorption coefficients for the six grains are quite consistent, showing a monotonic decrease from about 0.25 at 400 nm to about 0.12 at 700 nm (with

TABLE 5. Color values for filipstadite

Grain:	2			5			6			2			5			6		
	R_1	R_2	R'	R_1	R_2	R'	R_1	R_2	R'	mR_1	mR_2	${}^mR'$	mR_1	mR_2	${}^mR'$	mR_1	mR_2	${}^mR'$
	Illuminant C																	
x	0.3060	0.3055	0.3035	0.3059	0.3058	0.3028	0.3014	0.2980	0.3018	0.3015								
y	0.3112	0.3108	0.3089	0.3111	0.3113	0.3076	0.3061	0.3035	0.3069	0.3070								
Y (%)	11.7	11.8	12.3	11.4	11.5	2.27	2.34	2.53	2.15	2.21								
λ_d	473	474	475	473	474	474	475	477	475	476								
P_e (%)	2.1	2.3	3.3	2.2	2.2	3.7	4.4	5.9	4.1	4.2								
	Illuminant A																	
x	0.4438	0.4434	0.4416	0.4437	0.4436	0.4409	0.4397	0.4363	0.4400	0.4395								
y	0.4059	0.4058	0.4052	0.4059	0.4060	0.4048	0.4042	0.4036	0.4046	0.4048								
Y (%)	11.7	11.8	12.2	11.4	11.5	2.26	2.32	2.50	2.14	2.19								
λ_d	488	489	488	488	488	488	488	489	488	489								
P_e (%)	1.0	1.1	1.5	1.0	1.0	1.7	2.0	2.9	1.9	2.0								

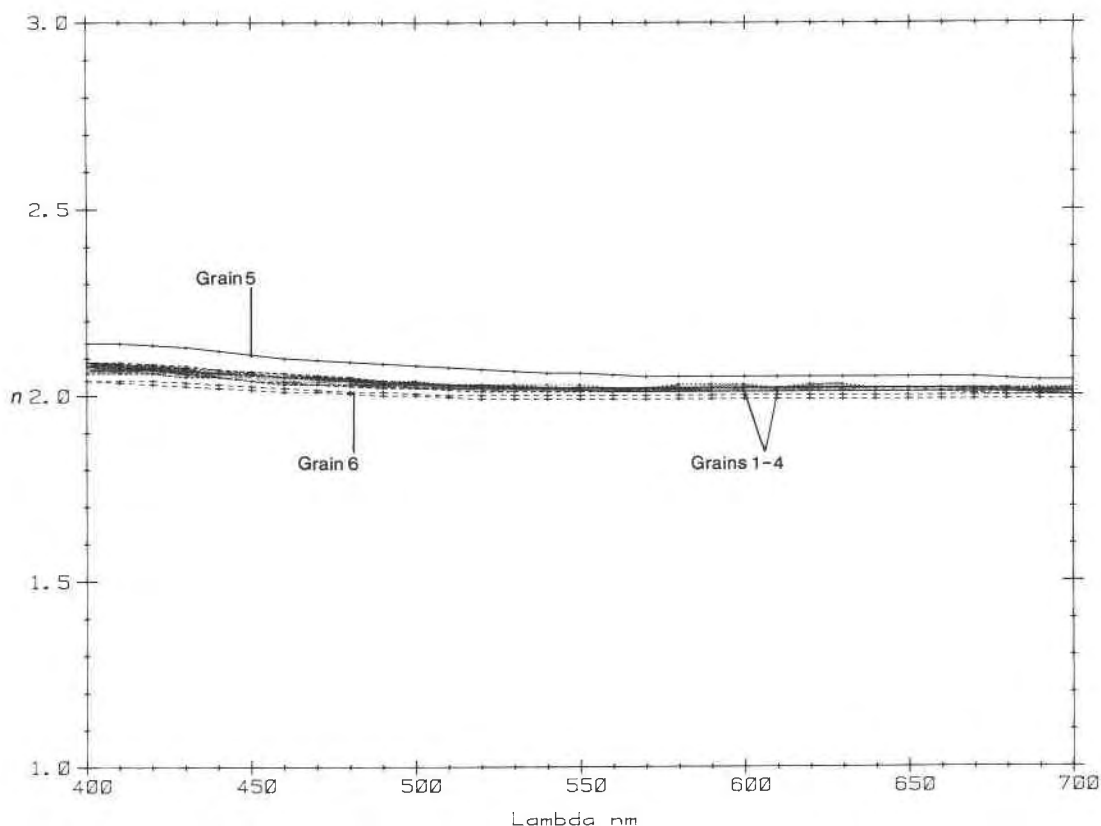


Fig. 7. Filipstadite: dispersion of the indices of refraction.

the exception of grain 1, which drops more rapidly to 0.02 at 700 nm), for the absorption $r < v$.

GLADSTONE-DALE RELATIONSHIP

The mean indices of refraction at 590 nm (Table 6; see footnote 1) were used with the appropriate densities calculated for the compositions (assuming the subcell to have $A = 8.640 \text{ \AA}$) to calculate K_p (physical refractive energy; Mandarino, 1979). Values for K_c (chemical refractive energy; Mandarino, 1979) were calculated from the compositional data in Table 2 using the revised Gladstone-Dale constants of Mandarino (1981). The two values were used to check the compatibility index (Mandarino, 1979) of filipstadite; on this scale, the results for grains 1 and 6 were in the "good" category, and those for grains 2 to 5 in the "excellent" category. It should be added that, in this instance, no allowance was made for the absorption coefficients of filipstadite.

COMPOSITION AND DISCUSSION

Filipstadite was analyzed using electron-microprobe techniques. Specific operating conditions, standards, and analyses are given in Table 2. The empirical formula, calculated for the average of analyses 1 to 4 and 6, and normalized to four oxygen atoms consistent with a spinel-type formula, is $\text{Mn}_{1.24}\text{Mg}_{0.74}\text{Al}_{0.03}\text{Fe}_{0.45}\text{Sb}_{0.51}\text{Si}_{0.01}\text{O}_4$.

Valence states of Mn, Fe, and Sb may all be multivalent. Sb is assumed to be Sb^{5+} , as only this valence is consistent with the octahedral-site coordinations in spinel. Charge balance requires that some Fe or Mn be oxidized. Because the formula will not balance with Fe^{3+} and Mn^{3+} and because oxidation potentials require that Fe be oxidized before Mn, we infer that Fe is present as Fe^{3+} and Mn^{2+} . This gives rise to the formula $(\text{Mn},\text{Mg})_2(\text{Sb}^{5+},\text{Fe}^{3+})\text{O}_4$.

Assuming that the detailed filipstadite structure has cation coordinations at least approximately equivalent to those in the parent spinel structure, the cations may be distributed over a single tetrahedrally and two octahedrally coordinated sites. There is no crystal-field stabilization energy for either Mn^{2+} or Fe^{3+} in either site. Essene and Peacor (1983) showed that the cation distribution in jacobsite, $\text{Mn}^{2+}\text{Fe}_3^{3+}\text{O}_4$, on which filipstadite may be overgrown, is probably normal. The usual coordination for Sb^{5+} is octahedral. Moore (1968) showed that melanostibite, $\text{Mn}(\text{Sb}_{0.5}^{5+}\text{Fe}_{0.5}^{3+})\text{O}_3$, is isostructural with ilmenite and has the ordered substitution $\text{Sb}^{5+} + \text{Fe}^{3+} = 2\text{Ti}^{4+}$, with Fe and Sb disordered over one set of octahedral sites. He emphasized that such substitutions may occur commonly. All of these relationships collectively imply that filipstadite has the ideal formula $\text{Mn}_2(\text{Sb}_{0.5}^{5+}\text{Fe}_{0.5}^{3+})\text{O}_4$, with Sb and Fe occupying octahedral sites and with Mg

substituting for Mn on the tetrahedrally coordinated sites. As noted above, ordering of Sb and Fe on octahedral sites is one possible source of the superstructure relations.

REFERENCES CITED

- Criddle, A.J., Stanley, C.J., Chisholm, J.E., and Fejer, E.E. (1983) Henryite, a new copper-silver telluride from Bisbee, Arizona. *Bulletin de Minéralogie*, 106, 511–517.
- Dunn, P.J., Peacor, D.R., Criddle, A.J., and Stanley, C.J. (1988) Ingeronite, a new calcium-manganese antimonate related to pyrochlore, from Långban, Sweden. *American Mineralogist*, 73, 405–412.
- Essene, E.J., and Peacor, D.R. (1983) Crystal chemistry and petrology of coexisting galaxite and jacobite and other spinel solid solutions and solvi. *American Mineralogist*, 68, 449–455.
- Hamilton, W.C. (1958) Neutron diffraction investigation of the 119° K transition in magnetite. *Physical Review*, 110, 1050–1057.
- Katz, G. (1960) Jacobite from the Negev, Israel. *American Mineralogist*, 45, 734–739.
- Mandarino, J.A. (1979) The Gladstone-Dale relationship. Part III: Some general applications. *Canadian Mineralogist*, 17, 71–76.
- (1981) The Gladstone-Dale relationship. Part IV: The compatibility concept and its application. *Canadian Mineralogist*, 19, 441–450.
- Moore, P.B. (1968) Substitutions of the type $(\text{Sb}_{0.5}^{\text{IV}}\text{Fe}_{0.5}^{\text{IV}}) = (\text{Ti}^{4+})$: The crystal structure of melanostibite. *American Mineralogist*, 53, 1104–1109.

MANUSCRIPT RECEIVED JUNE 19, 1987

MANUSCRIPT ACCEPTED NOVEMBER 20, 1987